

Beyond the Λ CDM cosmology: complex composition of dark matter.

M. Demiański^{1,2}, A.G. Doroshkevich³,

¹*Institute of Theoretical Physics, University of Warsaw, 00-681 Warsaw, Poland*

²*Department of Astronomy, Williams College, Williamstown, MA 01267, USA*

³*Astro Space Center of Lebedev Physical Institute of Russian Academy of Sciences, 117997 Moscow, Russia*

Accepted ..., Received ..., in original form

ABSTRACT

The mass and composition of dark matter (DM) particles and the shape of the power spectrum of density perturbations are estimated using recent observations of the DM dominated relaxed objects – dSph, THINGS and LSB galaxies and clusters of galaxies. We consider the most extensive available sample of observed objects with masses $10^6 \leq M_{\text{vir}}/M_{\odot} \leq 10^{15}$ which includes ~ 60 DM dominated galaxies and ~ 40 clusters of galaxies. We show that the observed characteristics of these objects are inconsistent with expectations of the standard Λ CDM cosmological model. However, they are well reproduced by a mixed CDM+WDM model with a significant contribution of the HDM-like power spectrum with a relatively large damping scale. We show that the central pressure of DM dominated objects is surprisingly weakly dependent upon their virial mass but it is very sensitive to the efficiency of cooling of the baryonic component. In contrast, the central entropy of both DM and baryonic components strongly depends upon the virial mass of halo and the period of halo formation. Unfortunately the available data prevent our qualitative approach to reach more reliable and definite conclusions which requires confrontation of more representative observational data with high resolution numerical simulations.

Key words: cosmology: composition of dark matter–formation of DM halos, galaxies and clusters of galaxies.

1 INTRODUCTION

The nature of dark matter (DM) particles is one of the intriguing questions of modern physics. These particles are an important element of the Standard Cosmology, they represent $\sim 20 - 25\%$ of the mean matter-energy density and explain some observed properties of the Universe (see, e.g., Komatsu 2011; Larson 2011; Burenin & Vikhlinin 2012; Saro 2013; Ade et al. 2013; Samushia et al. 2014). At the same time various candidates of DM particles are widely discussed as a very important element of high energy physics. This dual role of DM particles (see, e.g., Rubakov 2011) explains the great attention which is recently devoted to these problems. Many possible candidates of the DM particles are now considered. Thus, these particles may have masses ranging from massive gravitons with $m \sim 10^{-19} \text{ eV}$ and up to the supersymmetric WIMPs with $m \sim 10^{13} \text{ GeV}$. So wide range of possible masses is a result of very weak observational restrictions and implies similar wide range of other particle properties. In particular it is possible to note specially such traditional candidates as axino (Choi, Kim, Roszkowski 2013), or black holes (Carr 2014), and such exotic ones as

Atomic DM (Cyr-Racine & Sigurdson, 2013) and the flavor-mixed two component DM models (Medvedev 2014) or reincarnation of massive neutrino models (Costanzi et al. 2013; Villaescusa-Navarro et al. 2013). Very detailed discussion of various aspects of contribution of neutrinos to dark matter in the context of latest observations of Planck mission, baryonic oscillations and cluster properties can be found in Verde et al. (2013) and Wyman et al. (2014).

In turn the more and more refined observations determine evolution in time of the DM models. Historically in cosmology DM particles were introduced in Doroshkevich et al. (1980) and Bisnovaty-Kogan & Novikov (1980), as the Hot Dark Matter (HDM) model with the massive neutrino as the DM particles. Soon after the DM models were extended by introduction of the cold DM (CDM) and warm (WDM) models (Bond, Efstathiou & Silk, 1980; Bond & Szalay, 1983; Primack, 1984; Blumenthal et al., 1984; Bardeen et al. 1986) and even more complex models of multicomponent (MDM) and unstable DM particles (UDM) (Doroshkevich, Khlopov, 1984; Turner, Steigmann, Krauss, 1984; Doroshke-

vich, Khlopov, Kotok, 1986; Doroshkevich, Klypin, Khlopov, 1988).

All these models were solving some actual cosmological problems but their potential was always limited and none of them survived confrontation with observations. The scientific progress generates more problems and poses new questions what requires continuous modifications and development of new models of DM particles. Thus, early in this century observations of CMB fluctuations by the WMAP mission, SPT and other ground telescopes established the Λ CDM model as the best cosmological model (Bennet et al. 2003; Komatsu 2011; Larson 2011; Saro 2013). This inference was supported by Planck measurements (Ade et al. 2013), observations of clusters of galaxies (see, e.g., Burenin & Vikhlinin 2012) and baryonic oscillations (Eisenstein & Hu 1998; Meiksin et al. 1999; Samushia et al., 2014). At that time the main hope of identifying the “missing” cosmological components had been focused on links of possible distortions of the kinetic of recombination and the corresponding CMB fluctuations (see, e.g., Peebles et al. 2000; Doroshkevich et al. 2003).

On the other hand, for many years the emerging conflict between the Standard Λ CDM theory and observations of clustering on subgalactic scales is widely discussed. First, it is believed that the Λ CDM model predicts an excess of low-mass satellites of Milky Way, next is the core-cusp problem seen as a discrepancy between the observed and simulated shape of the density profiles in central regions of relaxed objects (see, e.g., Bovill & Ricotti, M., 2009; Koposov et al., 2009; Walker, & Penarrubia, 2011; Boylan-Kolchin et al., 2012; Penarrubia et al. 2012; Governato et al. 2012; Sawala, 2013; Teyssier et al. 2013; Laporte et al. 2013; Collins et al. 2014). Significance of these conflicts is quite moderate as objects with very different masses, densities and evolutionary histories are compared (see, e.g., Penarrubia et al. 2008). Moreover limited reliability of these contradictions is enhanced by limited resolution of both the observations and simulations (see, e.g., Mikheeva, Doroshkevich, Lukash 2007; Doroshkevich, Lukash & Mikheeva 2012; Pilipenko et al. 2012).

During last years the analysis of the $Ly - \alpha$ forest becomes very popular again (see, e.g. Boyarsky et al. 2009a,b, d; Dipak et al. 2012; Viel et al. 2013; Marcovič & Viel 2013; Borde et al. 2014). However information obtained in this way is also indirect and unreliable because there are many problems with measurements and especially with selection and interpretation of weak lines. Moreover properties of the $Ly - \alpha$ forest are very sensitive to the spatial variations of the poorly known UV background (Demiański et al. 2006; Kollmeier et al. 2014)).

Attempts of direct detection of DM particles by DAMA (Bernabei 2008, 2010), CRESST-II (Angloher et al. 2012), and SuperCDMS (Agnese 2013) experiments and others (see review in Gaitskill 2014) have not yet produced reliable positive results. Hence up to now we have no reliable estimates of the mass, the nature and properties of DM particles. However, the large amount of data already accumulated by the LHC could soon lead to detection of DM particles.

Now one of the most popular candidate for the DM particle is the sterile neutrino with a mass in the keV range (see, e.g., reviews of Feng 2010; Boyarsky et al., 2009c, 2013; Kusenko 2009; Kusenko & Rosenberg 2013; Drevs 2013;

Horiuchi et al. 2013; Marcovič & Viel 2013; Pontzen & Governato 2014). Sterile neutrinos can be produced during the inflation period or later via various processes. In particular a possible decay of some sort of sterile neutrinos is discussed (e.g., Ferrer & Hunter 2013; Bulbul et al. 2014; Boyarsky et al. 2014). So great diversity of possible properties and processes of generation of sterile neutrinos – from inflation and up to decays at some redshifts – eliminates correlations between the masses and velocities of these particles and increases uncertainties in expectations of their impact on the power spectrum and in particular on estimates of the damping scales. Let us note that the model with unstable DM particles implies also the multicomponent composition of DM.

It is believed that by modeling the three mentioned above effects namely, the $Ly - \alpha$ forest, density profile of DM dominated galaxies, the number of observed satellites of Milky Way, and observations of the high- z gamma-ray bursts (see e.g., reviews Boyarsky et al. 2009; Viel et al. 2013; Marcovič & Viel 2013; de Souza et al. 2013), it is possible to solve the problem of sterile neutrino and in particular to restrict its mass by $m_\nu \geq 10 - 20 \text{ keV}$. However these estimates restrict the damping scales and the shape of power spectrum rather than masses of DM particles (see, e.g., Tremaine & Gunn 1979; Ruffini et al. 2014). Recently X-ray emission with the energy $E \sim 3.5 \text{ keV}$ was detected from 73 galaxy clusters what can be interpreted either as a radiative decay of DM particles or as a recombination line of Ar (Bulbul et al. 2014; Boyarsky et al. 2014). A spatially extended excess of 1 – 3 GeV gamma rays from the Galactic Center could be related to annihilation of DM particles (Daylan et al. 2014; see also Modak et al. 2013). This discussion shows that now we do not have any reliable estimates of properties of DM particles.

The observations of DM dominated halos are very well complemented by numerical simulations which allow to trace and investigate the early stages of halos formation, as well as the process of halos virialization and formation of their internal structure. The formation of virialized DM halos begins as the anisotropic collapse in accordance with the Zel’dovich theory of gravitational instability (Zel’dovich 1970). During later stages the evolution of such objects becomes again more complex because it is influenced by their anisotropic environment (see, e.g., real cluster representations in Pratt et al. 2009). Moreover all the time the evolution goes through the process of violent relaxation and merging what is well reproduced by simulations.

Analysis of simulated halos can be performed in a wide range of halo masses and redshifts what allows to improve the description of properties of relaxed halos of galactic and cluster scales and to link them with the power spectrum of initial perturbations. Thus it is established that after a period of rapid evolution the main characteristics of majority of the high density virialized DM halos become frozen and their properties are only weakly changing owing to the accretion of diffuse matter and/or the evolution of their baryonic component. The basic properties of the relaxed DM halos are described in many papers (see, e.g., Tasitsiomi et al. 2004; Nagai et al. 2007; Croston et al. 2008; Pratt et al., 2009, 2010; Vikhlinin et al. 2006, 2009; Arnaud et al. 2010; Klypin et al. 2011; Kravtsov & Borgani 2012).

For the WDM model the available simulations (see, e.g., Maccio 2012, 2013; Angulo, Hahn, Abel, 2013; Schneider,

Smith & Reed, 2013; Wang et al. 2013; Libeskind et al. 2013; Marcovič & Viel 2013; Schultz et al. 2014; Schneider et al. 2014; Dutton et al. 2014) show that in accordance with expectations the number of low mass halos decreases and the central cusp in the density profile is transformed into the core. For larger halos the standard density profile is formed again but formation of high density objects is accompanied by appearance of some unexpected phenomena. Thus Maccio et al. (2012, 2013), Schneider et al. (2014) confirm the decrease of matter concentration in the WDM model in comparison with the CDM model but they inferred that 'standard' WDM model is not able to reproduce the density profile of low mass galaxies. This inference is enhanced in Libeskind et al. (2013) where in contrast with the CDM model their simulation with 1 keV WDM particles cannot reproduce the formation of the Local Group. In turn, Schultz et al. (2014) note that in their simulations with 3keV WDM particles formation of objects at large redshifts and reionization are oversuppressed. This means that the simulations of WDM and especially the multicomponent DM models require further detailed analysis and it is necessary to put special attention to reproduce links between the mass function of halos and the power spectra with the free streaming cut-off.

Without doubt, one can expect a rapid progress in simulations of more complex cosmological models. However for preliminary discussions of such models we can use the semi analytical description of DM dominated objects proposed in our previous paper (Demiański & Doroshkevich 2014). It is based on the approximate analytical description of the structure of collapsed halos formed by collisionless DM particles. During the last fifty years similar models have been considered and applied to study various aspects of nonlinear matter evolution (see, e.g., Peebles 1967; Zel'dovich & Novikov 1983; Fillmore and Goldreich 1984; Gurevich & Zybin 1995; Bryan & Norman 1998; Lithwick & Dalal 2011). Of course it ignores many important features of the process of halos formation and is based on the assumption that the virialized DM halo is formed during a short period of the spherical collapse at $z \approx z_f$ and later on its parameters vary slowly owing to the successive matter accretion (see, e.g., discussion in Bullock et al. 2001; Diemer et al. 2013).

Of course a spherical model can not adequately describe the real process of halos formation. However properties of the steady state virialized DM objects are mainly determined by the integral characteristics of protoobjects and are only weakly sensitive to details of their evolution. This is clearly seen in numerous simulations which show that the Navarro – Frenk – White (NFW) density profile (Navarro et al. 1995, 1996, 1997) very stably appears in majority of simulated DM halos.

The same simulations show also that properties of the central cores of virialized DM halos are established during the early period of halos formation and later on the slow pseudo-evolution of cores dominates. This means that properties of halo cores only weakly depend on the halo periphery and are determined mainly by their mass and the redshift of formation (Klypin et al. 2011). Using these results we formulate a rough two parametric description of all the basic properties of virialized DM halos. These two basic parameters are the virial mass of halos and the redshift of their formation. Of course, they actually characterize the initial

entropy of compressed DM particles and its growth in the process of violent relaxation of the compressed DM component. But this approach allows us also to reveal a close correlation between the central pressure and density of DM halos and the initial power spectrum of density perturbations.

Of course this approach is applied for the DM dominated halos only as the dissipative evolution of the baryonic component distorts properties of the cores of DM halos. Thus we can use this model in two ways:

(i) We can use the central density and pressure of the DM component and redshift of the DM halos formation, z_f , as a parameter that characterizes the 'frozen' properties of the central region of DM halos. This redshift of formation correlates also with the virial mass of halos and with the initial power spectrum.

(ii) Application of the Press – Schechter (1974) approach allows us to link together data obtained for a wide range of mass of virialized objects and thus to restrict the shape of the initial power spectrum and some characteristics of the DM particles.

However potential of this approach should not be overestimated. As usual we can only determine the probability of object formation and therefore they have statistical character rather than strict constraints or predictions. Moreover in our discussion we use observational data of only limited quality and representativity. Thus we can use only small number (≤ 100) of the observed DM dominated objects, their observed characteristics – even so important as the virial mass – are known only with very limited precision and significant scatter. None the less the potential of the proposed approach is significant as it considers objects in a wide range of masses. We hope that further accumulation of observational data and their comparison with the high resolution simulations will allow to essentially improve presented results.

This paper is organized as follows: In Sec. 2 the basic model, relations and assumptions of our approach are formulated. In Sec. 3 a short description of an approximate model of DM dominated halo is presented. Characteristics of the observed DM dominated objects – galaxies and clusters of galaxies – are described in Secs. 4 and 5, and in Sec. 6 properties of the central entropy and pressure of DM dominated virialized objects are discussed. Some possible MDM models are presented in Sec. 7. Discussion and conclusions can be found in Sec. 8.

2 COSMOLOGICAL MODELS WITH THE CDM, WDM AND MULTI COMPONENT DM

2.1 Cosmological parameters

In this paper we consider the spatially flat Λ dominated model of the Universe with the Hubble parameter, $H(z)$, the mean critical density $\langle\rho_{cr}\rangle$, the mean density of non relativistic matter (dark matter and baryons), $\langle\rho_m(z)\rangle$, and the mean density and mean number density of baryons, $\langle\rho_b(z)\rangle$ & $\langle n_b(z)\rangle$, given by Komatsu et al. (2011), Hinshaw et al. (2013):

$$H^2(z) = H_0^2[\Omega_m(1+z)^3 + \Omega_\Lambda], \quad H_0 = 100h \text{ km/s/Mpc},$$

$$\langle \rho_m(z) \rangle = 2.5 \cdot 10^{-27} z_{10}^3 \Theta_m \frac{g}{\text{cm}^3} = 3.4 \cdot 10^4 z_{10}^3 \Theta_m \frac{M_\odot}{\text{kpc}^3},$$

$$\langle \rho_b(z) \rangle = \frac{3H_0^2}{8\pi G} \Omega_b (1+z)^3 \approx 4 \cdot 10^{-28} z_{10}^3 \Theta_b \frac{g}{\text{cm}^3}, \quad (1)$$

$$\langle \rho_{cr} \rangle = \frac{3H^2}{8\pi G}, \quad z_{10} = \frac{1+z}{10}, \quad \Theta_m = \frac{\Omega_m h^2}{0.12}, \quad \Theta_b = \frac{\Omega_b h^2}{0.02}.$$

Here $\Omega_m = 0.24$ & $\Omega_\Lambda = 0.76$ are the mean dimensionless density of non relativistic matter and dark energy, $\Omega_b \approx 0.04$ and $h = 0.7$ are the dimensionless mean density of baryons, and the Hubble constant measured at the present epoch. Cosmological parameters presented in the recent publication of the Planck collaboration (Ade et al. 2013) slightly differ from those used above (1).

For this model the evolution of perturbations can be described with sufficient precision by the expression

$$\delta\rho/\rho \propto B(z), \quad B^{-3}(z) \approx \frac{1 - \Omega_m + 2.2\Omega_m(1+z)^3}{1 + 1.2\Omega_m}, \quad (2)$$

(Demiański, Doroshkevich, 1999, 2004, 2014; Demiański et al. 2011) and for $\Omega_m \approx 0.25$ we get

$$B^{-1}(z) \approx \frac{1+z}{1.35} [1 + 1.44/(1+z)^3]^{1/3}. \quad (3)$$

For $z = 0$ we have $B = 1$ and for $z \geq 1$, $B(z)$ is reproducing the exact value with accuracy better than 90%.

For $z \gg 1$ these relations simplify. Thus, for the Hubble constant and the function $B(z)$ we get

$$H^{-1}(z) \approx \frac{2.7 \cdot 10^{16}}{\sqrt{\Theta_m}} s \left[\frac{10}{1+z} \right]^{3/2}, \quad B(z) \approx \frac{1.35}{1+z}. \quad (4)$$

2.2 Power spectrum in the WDM models

The transfer function for the WDM model with thermalized DM particles was obtained by Bode, Ostriker and Turok (2001) and more recently in Viel et al. (2005) (see also Polisensky & Ricotti 2011; Marcovič & Viel 2013). In these papers the transfer function was written as

$$T_{WDM} \approx [1 + (\alpha_w q)^{2.25}]^{-4.46}, \quad (5)$$

$$q = \frac{k}{\Omega_m h^2} \text{Mpc}, \quad \alpha_w = 6 \cdot 10^{-3} \left(\frac{\Omega_m h^2}{0.12} \right)^{1.4} \left(\frac{1 \text{keV}}{m_w} \right)^{1.1},$$

where k is the comoving wave number.

The correlation function of the density perturbations

$$\sigma_m^2(R) = 4\pi \int_0^\infty p(k) W^2(kR) k^2 dk, \quad (6)$$

with the standard top-hat window function $W(kR)$ has been discussed already many years ago (see, e.g., Loeb & Barkana, 2001). Following the Press – Schechter approach (Press & Schechter 1974; Peebles 1974; Peacock & Heavens 1990; Bond et al. 1991; Mantz et al. 2010) we can link the redshift of formation z_f of virialized objects with mass M_{vir} with the correlation function $\sigma_m(M_{vir})$ by the condition

$$B(z_f) \sigma_m(M_{vir}) \approx \text{const}. \quad (7)$$

However this approach does not allow us to obtain an independent estimate of the small scale amplitude of perturbations. More detailed comparison of the mass dependence of the redshift of formation of galaxies and clusters of galaxies

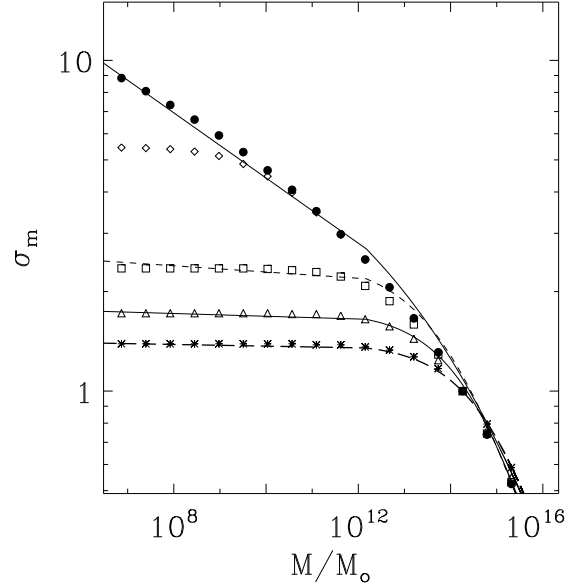


Figure 1. Correlation functions of the matter density σ_m are plotted vs. the virial mass of objects, M_{vir}/M_\odot , for the CDM power spectrum (Bardeen et al. 1986) (points) and for the WDM power spectrum (5) with $m_w = 1, 0.1, 0.05$, & 0.03keV (rhombus, squares, triangles and stars). Fits (9), and (11) are plotted by solid lines, fits (8) and (10) are plotted by dashed and long dashed lines.

requires much more precise estimates of the observational parameters of both galaxies and clusters of galaxies. In particular thus defined σ_m depends upon the shape of the transfer function (5) and for the MDM model more accurate determination of this function is required.

For the transfer function (5) the correlation function of the density fluctuations is plotted in Fig. 1 for four values of $m_w = 1, 0.1, 0.05$, & 0.03keV and can be fitted with reasonable precision by the expressions

$$\sigma_m(M) = 2.5/(1 + 0.12M_{12}^{0.45}), \quad m_w = 0.1 \text{keV}, \quad (8)$$

$$\sigma_m(M) = 1.8/(1 + 0.05M_{12}^{0.45}), \quad m_w = 0.05 \text{keV}, \quad (9)$$

$$\sigma_m(M) = 1.4/(1 + 0.03M_{12}^{0.45}), \quad m_w = 0.03 \text{keV}. \quad (10)$$

For comparison in the same Figure the correlation function for the standard CDM model is also plotted. It is well fitted by the expression (Klypin et al., 2011):

$$\sigma_m(M) = 3.9M_{12}^{-0.077}/(1 + 0.18M_{12}^{0.133} + 0.14M_{12}^{0.333}). \quad (11)$$

As is seen from Fig. 1 for the mass of the WDM particles $m_w \geq 1 \text{keV}$ functions σ_m differ from the CDM one for objects with moderate mass $M_{vir} \leq 10^9 M_\odot$ only. For the WDM model with less massive particles $1 \text{keV} \geq m_w \geq 0.03 \text{keV}$ the damping mass falls in the range $10^{10} \leq M_{vir}/M_\odot \leq 10^{14}$. Such damping strongly decelerates formation of objects with mass $M_{obj} \leq M_{dmp}$ (see, e.g., Schultz et al. 2014).

2.3 Power spectrum in MDM models

The evolution of perturbations in MDM models was discussed many times in different approximations (see e.g. Grishchuk & Zel'dovich 1981; Turner et al. 1984; Doroshkevich et al. 1984; Boyarsky et al. 2009b; Anderhalden et al. 2012).

It is important that in contrast with the CDM or WDM models with one mass of particles in MDM models the shape of transfer function is time dependent. Indeed even relatively small fraction of WDM particles with $m_w \leq m_{cdm}$ significantly decelerates the growth of CDM perturbations at small scales as compared with the standard CDM model. This deceleration decreases with time the height of plateau in the transfer function of MDM model for larger k what leads to the progressive damping of the power spectrum at such scales. This problem was briefly discussed by Boyarsky et al. (2009b) where the contribution of the CDM power spectrum, g_{cdm} , to the full power spectrum at redshifts $z \leq 1$ is roughly linked with the fraction of CDM matter f_{cdm} as

$$g_{cdm} \approx f_{cdm} 10^{2.58(1-f_{cdm})}. \quad (12)$$

This fit neglects the time dependence of the height of plateau in the MDM transfer function what misrepresents the shape of the MDM power spectrum and the function $\sigma_m(M_{vir})$ and thus increases uncertainties of our consideration. Non the less allowing for qualitative character of our approach, further on, we will use this relation to roughly link the spectral and matter fractions, g_{cdm} and f_{cdm} . Unfortunately we do not see a simple way to improve on these disadvantages and in what follows we will determine the MDM correlation function by the relation

$$\sigma_m(M) = \sqrt{g_{cdm}\sigma_{cdm}^2 + g_{wdm}\sigma_{wdm}^2}. \quad (13)$$

This relation implies statistical independence of perturbations in the CDM and WDM mediums what is only approximately correct. More precise conclusions can be obtained with high resolution numerical simulations.

3 PHYSICAL MODEL OF HALOS FORMATION

Properties of both simulated and observed virialized objects – galaxies and clusters of galaxies – are usually described in the framework of spherical models such as Navarro – Frenk – White (NFW) (Navarro et al. 1995, 1996, 1997; Ludlow et al. 2013), Burkert (1995) or isothermal models. In this paper we link the virial mass of DM halos M_{vir} with the redshift of their formation, z_f . For this purpose we use the spherical model of DM halos formation which was discussed in many papers (see, e.g., Peebles 1967, Umemura et al., 1993, Bryan & Norman 1998). Here we will briefly describe the main properties of this model.

It is commonly accepted that in the course of complex nonlinear condensation the DM forms stable virialized halos with a more or less standard density profile. Numerical simulations show that the virialized DM halos are formed from initial perturbations after a short period of rapid complex evolution. For example such virialized objects are observed as isolated galaxies and/or as high density galaxies embedded within clusters of galaxies, filaments, superclusters or other elements of the Large Scale Structure of the Universe. This approach also allows us to estimate the redshift when the observed DM dominated objects such as the dSph galaxies and clusters of galaxies were formed. Of course, this model ignores all details of the complex process of halos formation. But it allows to obtain a very simple, though

rough, description of this process and introduces some order of objects formation.

Our simple physical model of halos formation is based on the following assumptions:

(i) We assume that at redshift $z = z_f$ the evolution of DM perturbations results in the formation of spherical virialized DM halos with masses $M_{vir} = M_{13} \cdot 10^{13} M_\odot$ and the central densities ρ_c .

(ii) We do not discuss the dynamics of DM halos evolution which is accompanied by the progressive matter accretion, the growth of the halos masses and corresponding variations of other halos parameters. The real process of halos formation is extended in time what causes some ambiguity in their parameters such as the halos masses and the redshift of their formation (see, e.g. discussion in Diemand, Kuhlen & Madau 2007; Kravtsov & Borgani 2012). In the proposed model the redshift of halo formation, z_f , is identified with the redshift of collapse of the homogeneous spherical cloud with the virial mass M_{vir} ,

$$1 + z_f \approx 0.63(1 + z_{tr}), \quad (14)$$

where z_{tr} is the redshift corresponding to the turn around moment of the dust cloud evolution (see discussion of spherical model in Umemura, Loeb & Turner 1993).

(iii) We assume that in the course of DM halo formation the main fraction of the baryonic component is heated by the accompanied shock waves up to the temperature and pressure comparable with the virialized values of the DM component. These processes are responsible for the formation of equilibrium distribution of the baryonic component.

(iv) We assume that some (random) fraction of the compressed baryons is collected into a system of subclouds which are rapidly cooled and transformed into high density subclouds. Thus, the virialized halo configuration is composed of the DM particles, the hot low density baryonic gas, and cold high density baryonic subclouds.

(v) Transformation of less massive DM halos into the first observed galaxies with some fraction of stars was discussed in (Demiański & Doroshkevich 2014).

The evolution of the cooled subclouds can be very complex. It can be approximated by the isobaric mode of the thermal instability and therefore it does not preserve the compact shape of the cooled subclouds. As was discussed in Doroshkevich and Zel'dovich (1981) the motion of such subclouds within the hot gas leads to their deformation and less massive subclouds could be disrupted and even dissipated. The complex aspherical shape of such subclouds makes their survival problematic and requires very detailed investigation to estimate their evolution even in simulations. These problems are however beyond the scope of this paper.

The basic parameters of the discussed model – the virial mass, M_{vir} , central density, ρ_c , and concentration, C , connect the central and mean densities of objects by expressions

$$M_{vir} = 4\pi/3 R_{vir}^3 \Delta_v \langle \rho_{cr}(z_f) \rangle = 4\pi \rho_c R_{vir}^3 C^{-3} f_m(C), \quad (15)$$

$$\frac{C^3(z_f, M_{vir})}{f_m(C)} = \frac{3\rho_c}{\Delta_v \langle \rho_{cr}(z_f) \rangle}, \quad f_m = \int_0^C dx x^2 \frac{\rho(x)}{\rho_c}, \quad (16)$$

$$C = R_{vir}/r_c, \quad x = r/r_c, \quad \Delta_v = 18\pi^2 \approx 200.$$

Here R_{vir} and r_c are the virial radius of halo and the ra-

dius of central core (for the NFW or Burkert (1995) models) or size of the isothermal core, ρ_c and $\langle \rho_{cr}(z_f) \rangle$ are the central density of halo and the critical density of the Universe at redshift z_f (1). The value of mean overdensity, Δ_v , was derived from the simple model of spherical collapse that ignores the influence of complex anisotropic halos environment (see, e.g., Bryan & Norman 1998; Vikhlinin et al. 2009; Lloyd-Davies et al. 2011). The well known factor $f_m(C) \sim 1$ links the virial mass of an object with its concentration. Impact of the factor $f(C)$ can be determined by the method of successive approximations using, for example, the NFW density profile with

$$f_m(C) = \ln(1+C) - C/(1+C),$$

or quite similar expression for the Burkert (1995) model.

Application of this approach is possible for a given concentration $C(z_f, M_{vir})$. Below in section 4 we will use suitable fits for $C(z_f, M_{vir})$ given by Klypin et al. (2011).

Of course, this approach provides the qualitative description only and has limited predictive power. Thus, it ignores the complex anisotropic successive matter compression within filaments and walls before formation of compact halos, it ignores the effects produced by mergers, by anisotropic halo environment and so on. More detailed description can be achieved in the framework of more complex aspherical model which would take into account possible impact of such ignored effects as a random scatter of redshift of halos formation and other halo characteristics for a given virial mass. However use of such more complex models is not verified and direct comparison of observed and simulated objects seems to be more successful.

In central regions of halos the gas pressure is supported by adiabatic inflow of high entropy gas from outer regions of halos what leads to progressive concentration of baryonic component within central regions of halos and to formation of massive baryonic cores (see, e.g. Wise & Abel 2008; Pratt et al. 2009; McDonald et al. 2013).

4 OBSERVED CHARACTERISTICS OF CLUSTERS OF GALAXIES

For our analysis we use more or less reliable observational data for ~ 150 DM dominated clusters of galaxies, for ~ 40 dSph, and ~ 20 other DM dominated galaxies. The analysis of observations of the dSph galaxies in the framework of accepted model was performed in Demiański & Doroshkevich (2014). Here we continue this analysis and compare observational results with theoretical expectations.

4.1 Redshift of formation of clusters of galaxies

Now there are more or less reliable observational data at least for ~ 300 clusters of galaxies (Pointecouteau et al. 2005; Arnaud et al., 2005; Pratt et al., 2006; Zhang et al., 2006; Branchesi et al., 2007; Vikhlinin et al., 2009; Pratt et al. 2010; Suhada et al. 2012; Moughan et al. 2012; Foëx et al. 2013; Bhattacharya et al. 2013). However, the central cluster characteristics are not directly observed and are obtained by a rather complex procedure (see, e.g., Bryan & Norman 1998; Vikhlinin et al. 2009; Lloyd-Davies et al. 2011; McDonald et al., 2013).

In spite of the speedy progress in investigations of the clusters of galaxies recent publications discuss mainly the observations of general cluster characteristics such as their redshift z_{obs} , virial mass, M_{vir} , radius, R_{vir} , and average temperature, T_x . It is important that only the observed redshift of clusters, and their averaged temperature are really measured while other characteristics are usually derived using empirical correlations (see, e.g., Pointecouteau et al. 2005; Vikhlinin et al., 2006; Nulsen, Powell, & Vikhlinin, 2010). It is interesting that some of these correlations can be expressed in the standard form used for description of virialized objects,

$$\beta = \frac{U}{W} \approx \frac{GM_{vir}}{R_{vir}T_x} = const,$$

where U & W are the gravitational and internal energy of the object. Thus for 179 observed clusters with masses $2 \leq M_{13} = M_{vir}/10^{13} M_\odot \leq 250$ we have

$$\langle \beta \rangle = \left\langle \frac{M_{13}}{R_{Mpc} T_{kev}} \right\rangle \approx 7.16(1 \pm 0.08). \quad (17)$$

In spite of limited precision of these determinations small scatter of β demonstrates both stability of observational methods and similarity of internal structure of clusters.

However in this paper we are mainly interested in discussion of more stable central regions of clusters and, in particular, in concentrations and in the central pressure of clusters. Unfortunately the body of such data is very limited.

In this section we consider properties of the central regions of virialized DM halos using the approximation presented in Klypin et al. (2011), Prada et al. (2012), Angulo et al. (2012). We characterize halos by their virial mass M_{vir} and redshift of formation, $z = z_f$. We assume that at $z \leq z_f$ the halos mass and mean temperature and density remain almost the same and as usual we take

$$\langle \rho_{cl}(z_f) \rangle \simeq 500 \rho_m(z_f) \approx 1.25 \cdot 10^{-27} (1 + z_f)^3 g/cm^3. \quad (18)$$

The mean baryonic number density of relaxed halos is

$$\langle n_b(z_f) \rangle = 1.5 \cdot 10^{-4} (1 + z_f)^3 \Theta_b cm^{-3}.$$

4.2 Observed characteristics of clusters formed at small redshifts

For clusters of galaxies with mass $M_{vir} = M_{13} \cdot 10^{13} M_\odot$ formed at redshifts $z \leq 1$ the concentration $C(M_{vir}, z_f)$ is given by the expression (Klypin et al. 2011)

$$C(M_{vir}, z_f) \approx 7.5 B^{4/3} (z_f) M_{13}^{-0.09}, \quad (19)$$

and for such clusters determination of the redshift z_f is difficult. Indeed, comparison of the central density $\rho_c(M_{vir}, z_f)$ with the mean density shows that,

$$\rho_c(M, z_f) \approx \frac{\langle \rho_{cl} \rangle C^3}{3 f_m(C)} \approx 1.8 \cdot 10^{-25} \frac{g}{cm^3} \frac{D^3(z_f)}{M_{13}^{0.27} f_m(C)},$$

$$n_c(M, z_f) \approx 0.1 M_{13}^{-0.27} cm^{-3} D^3(z_f) / f_m(C), \quad (20)$$

$$D(z_f) = (1 + z_f) B^{4/3} (z_f),$$

and the function $f_m(C) \sim 1$ was introduced by (16). It is important that $D(z)$ only very weakly depends on the redshift, $D(z) \sim 1.1$ for $0 \leq z \leq 1$ and the precision of available

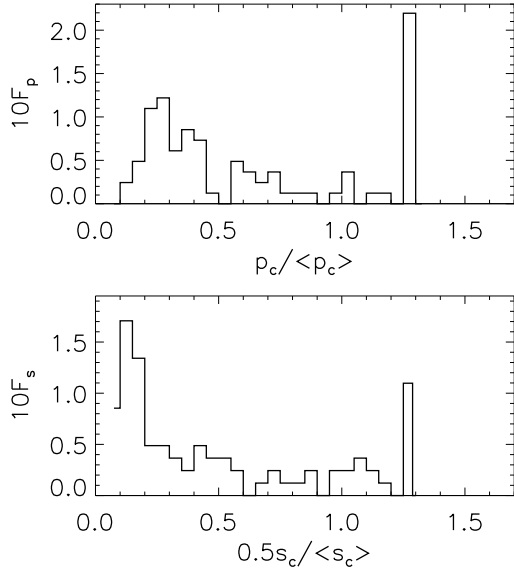


Figure 2. For 83 clusters from the SPT-sample the distribution functions of the central pressure, $F_p(p_c/\langle p_c \rangle)$ and central entropy $F_s(0.5s_c/\langle s_c \rangle)$ are plotted.

data set makes it difficult to reveal evolution of clusters and to use them for discussion of cosmological problems.

For 18 nearby clusters observed at $\langle z_{obs} \rangle = 0.095$ and with masses $8 \leq M_{13} \leq 120$ (Pointecouteau 2005; Vikhlinin 2006; Bhattacharya et al. 2013) the measured values of concentration are

$$\langle C \rangle = 3.46(1 \pm 0.15), \quad f_m(C) \approx 0.73.$$

These data allow us to roughly estimate the central pressure, P_c , baryon number density, n_c , and entropy, S_c in clusters and the redshift of their formation as

$$\langle P_c \rangle \approx 23.1(1 \pm 0.5) \text{ eV/cm}^3, \quad (21)$$

$$\langle n_c \rangle \approx 0.5 \cdot 10^{-2} (1 \pm 0.5) \text{ cm}^{-3}, \quad \left\langle \frac{1+z_f}{1+z_{obs}} \right\rangle \approx 1.66,$$

$$\langle S_b \rangle = \langle P_c/n_c^{5/3} \rangle \approx 180(1 \pm 0.7) \text{ cm}^2 \text{ keV}, \quad (22)$$

$$\langle 1+z_f \rangle \approx 1.8(1 \pm 0.2), \quad \langle B^{-1}(z_f) \rangle \approx 1.5(1 \pm 0.14). \quad (23)$$

These results confirm that clusters are formed earlier than they are observed and it is necessary to bear in mind this difference in the course of interpretation of cluster parameters.

4.3 Properties of the DM halos formed at larger redshifts

4.3.1 Theoretical expectations

For description of galactic scale halos or earlier formed DM halos of cluster scale it is convenient to use other approximation of halo parameters (Klypin et al. 2011; Demiański & Doroshkevich, 2014)

$$C \approx 0.18 M_{13}^{1/6} (1+z_f)^{7/3} = 0.18 M_{13}^{-1/15} \eta^{7/3}, \quad (24)$$

$$\eta = (1+z_f) M_{13}^{0.1}.$$

Comparison with observations shows that for the DM dominated relaxed objects

$$\eta \sim 3.2 - 3.3, \quad (25)$$

remains almost the same in a wide range of virial masses and redshifts z_f . For such halos using (16) and (24) we expect to have for the central density of the DM matter

$$\rho_c(M, z) \approx \rho_0 (1+z_f)^{10} M_{13}^{1/2} = \rho_0 \eta^{10} M_{13}^{-1/2}, \quad (26)$$

$$\rho_0 = 1.1 \cdot 10^{-8} \Theta_\rho \frac{M_\odot}{pc^3}, \quad \Theta_\rho = \frac{\delta_r}{f_m(C)} \frac{\Delta_v}{200} \Theta_m,$$

and for the central baryonic number density

$$n_b = 0.14 \text{ cm}^{-3} (\eta/3.3)^{10} M_{13}^{-1/2} \Theta_b \Theta_\rho. \quad (27)$$

Here Θ_ρ describes the random variations of the central density (δ_r) and uncertainties in determination of the observed parameters. As was shown in Demiański & Doroshkevich (2014) for the concentration (24) the central pressure depends only upon $\eta(M_{vir}, z_f)$ (25) and we get

$$P_c(M_{vir}, z_f) \approx P_0 (\eta/3.3)^{40/3}, \quad P_0 \approx 28 \text{ eV/cm}^3. \quad (28)$$

It can be expected that it is only weakly sensitive to other parameters of clusters. For the central entropy we get

$$S_c = P_c/n_b^{5/3} \approx 0.76 (3.3/\eta)^{10/3} M_{13}^{5/6} \text{ cm}^2 \text{ keV}. \quad (29)$$

4.3.2 Properties of SPT clusters

These expectations can be compared with parameters of 83 clusters selected by the South Pole Telescope (Reinhardt et al. 2013; McDonald et al. 2013; Ruel et al. 2013; Salwanchik et al. 2013). For this SPT-sample of clusters the central baryonic density, temperature and entropy are given at radius $r \leq 0.012 R_{500}$ where R_{500} is the radius of a sphere within which the average density is $500 \rho_{crit}(z_{abs})$. For 31 clusters also standard X-ray masses derived from Chandra observations (Ruel et al. 2013) are known.

For this sample the distribution functions of the central pressure and entropy are plotted in Fig. 2 where

$$\langle P_c \rangle \approx 146 \text{ eV/cm}^3, \quad \langle S_c \rangle \approx 145 \text{ keV cm}^2. \quad (30)$$

As is seen from this Figure this sample is clearly divided into two groups. One of them contains 39 clusters with higher central pressure and low entropy

$$\langle P_{col} \rangle = 270 \text{ eV/cm}^3, \quad \langle S_{col} \rangle = 100 \text{ keV cm}^2. \quad (31)$$

For these clusters both the baryonic density and pressure are extremely high, while the entropy is small. This is explained by strong cooling and clumping of the observed gaseous component. It can be expected that in these clusters owing to the thermal instability the baryonic matter forms two fractions, one of which is represented by a system of high density low temperature clouds and the other is composed of high temperature low density gas. In this case the measured density relates to the denser fraction while the temperature relates to the hot gas and random velocities of clouds (see, e.g., Khedekar et al. 2013). If this interpretation is correct then the measured P_c and S_c (31) are artificial and the real central pressure and entropy of the hot component are close to that measured for the other 44 clusters presented below while the entropy of the cold component is less than (31).

For the subsample of 44 clusters with $1 \leq M_{13} \leq 100$ and moderate central pressure $P_c \leq 70 \text{ eV/cm}^3$, we have

$$\langle P_c \rangle \approx 36.1(1 \pm 0.37) \text{ eV/cm}^3, \quad \eta \approx 3.36(1 \pm 0.04), \quad (32)$$

$$\kappa(n_c, T_c) \approx -0.67,$$

where $\kappa(f_1, f_2)$ is the standard correlation coefficient

$$\kappa(f_1, f_2) = (\langle f_1 f_2 \rangle - \langle f_1 \rangle \langle f_2 \rangle) / \sigma_1 \sigma_2. \quad (33)$$

However this subsample is naturally divided into two groups. Hotter group accumulates 24 clusters with

$$\langle n_c \rangle = 0.5 \cdot 10^{-2} (1 \pm 0.4) \text{ cm}^{-3}, \quad \kappa(n_c, T_c) \approx -0.65,$$

$$\langle P_c \rangle \approx 36.2(1 \pm 0.35) \text{ eV/cm}^3, \quad \langle T_c \rangle = 7.8(1 \pm 0.3) \text{ keV}, \quad (34)$$

$$\langle S_b \rangle = 305(1 \pm 0.5) \text{ cm}^2 \text{ keV}, \quad \kappa(P_c, S_b) = -0.2.$$

For 20 colder clusters we get

$$\langle n_c \rangle = 1.8 \cdot 10^{-2} (1 \pm 0.6) \text{ cm}^{-3}, \quad \kappa(n_c, T_c) \approx -0.54,$$

$$\langle P_c \rangle \approx 35.9(1 \pm 0.39) \text{ eV/cm}^3, \quad \langle T_c \rangle = 2.3(1 \pm 0.4) \text{ keV}, \quad (35)$$

$$\langle S_b \rangle = 41(1 \pm 0.6) \text{ cm}^2 \text{ keV}, \quad \kappa(P_c, S_b) = -0.1.$$

The noticeable correlation of the cluster temperature and density together with negligible correlation between cluster pressure and entropy allows to obtain more detailed description of the process of DM compression and successive violent relaxation of the compressed matter. As is seen from (34, 35) both the central pressure and entropy contain some regular term depending upon characteristics of clusters (for (34)) and upon cooling of baryonic component (for (35)). The random fluctuations of the pressure and entropy, $\delta P_c / P_c$ & $\delta S_c / S_c$, with

$$\sigma_p^2 = \langle (\delta P_c / P_c)^2 \rangle \approx 0.16, \quad \sigma_s^2 = \langle (\delta S_c / S_c)^2 \rangle \approx 0.3,$$

are (almost) independent. Neglecting their correlation, $\kappa(P_c, S_b) = 0$, it is easy to see that the dispersions of the central density, σ_n , and temperature, σ_T , and their correlation coefficient, $\kappa(n_c, T_c)$, are simple functions of σ_p & σ_s . Indeed, for $P_c = S_b n_c^{5/3} = T_c n_c$

$$\sigma_n = 0.6 \sqrt{\sigma_p^2 + \sigma_s^2} \sim 0.45, \quad \sigma_T = 0.6 \sqrt{0.44 \sigma_p^2 + \sigma_s^2} \sim 0.36,$$

$$\kappa(n_c, T_c) \approx -0.6, \text{ for } \sigma_p / \sigma_s \approx 0.7,$$

what is comparable with (34, 35). These properties of perturbations seem to suggest that uncorrelated pressure and entropy perturbations are fundamental while perturbations of density and temperature can be considered as their consequence.

The differences in properties of 24 hotter and 20 colder clusters could be mainly caused by cooling of the baryonic component. Indeed, the isobaric thermal instability results in formation of a two phase medium – cold denser clouds moving within hot gas – but it does not perturb the gas pressure. Weak scatter of the central pressure of these clusters (32) shows that this pressure as well as the entropy of 24 hot clusters characterize the regular process of violent relaxation of the dominant DM component while the decrease of entropy for 20 colder clusters is naturally explained by the cooling of baryonic component. The random uncorrelated scatter of the central pressure and entropy are naturally related to random uncorrelated variations in the initial state of the compressed matter.

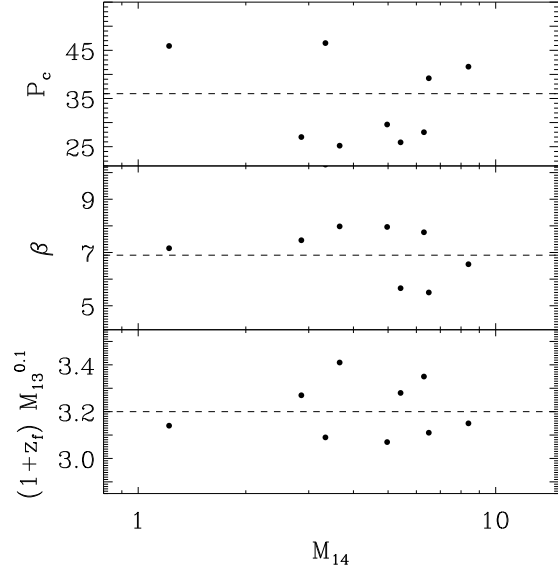


Figure 3. For 9 clusters from the SPT-sample the virial factor $\beta = M_{13}/R_{vir}/T$, redshift creation, $1 + z_f$ and central pressure, $P_c \text{ eV/cm}^3$ are plotted vs. the masses M_{14} . Fits (36, 37, & 38) are plotted by dashed lines

For 9 clusters of this subsample also their X-ray mass was determined. For these clusters with $10 \leq M_{13} \leq 80$ and

$$\langle \beta \rangle = \left\langle \frac{M_{13}}{R_x T_x} \right\rangle \approx 8(1 \pm 0.18), \quad \langle 1 + z_{obs} \rangle = 1.7(1 \pm 0.12), \quad (36)$$

we get for the pressure, P_c & η , baryonic number density, n_b , and the entropy, S_b :

$$\langle n_b \rangle \approx 0.7 \cdot 10^{-2} (1 \pm 0.4) \text{ cm}^{-3},$$

$$\langle P_c \rangle \approx 34.2(1 \pm 0.24) \text{ eV/cm}^3, \quad (37)$$

$$\langle \eta \rangle \approx 3.35(1 \pm 0.02),$$

$$\langle S_b \rangle = 200(1 \pm 0.7) \text{ cm}^2 \text{ keV}.$$

It is important that if the central pressures of both subsamples (34) and (35) are close to the expected one (28) then the observed central entropies (34) and (35) noticeably exceed the expected value (29). Reasons of these divergences are unknown but it can be expected that the progressive growth of small scale perturbations and their following randomization can sufficiently increase the large scale entropy of matter compressed in clusters of galaxies. This problem requires further analysis in simulations.

The redshift of cluster formation, z_f can be determined by two methods. Firstly, we could use the measurements of the baryonic number density and find the concentration, C , and z_f from (16) and (26). However, the n_c & T_c are observed at the radius $r \sim 0.012 R_{vir}$, where radial variations of density and temperature can be significant, what generates additional uncertainties in the estimated value of z_f . One can also use measurements of pressure and parameter η from (28). In central regions of DM halos radial variations of pressure are small, scatter of η is negligible and therefore precision of so determined z_f depends mainly on the precision of measurements of the cluster mass, M_{13} , in Eq. (25).

Using the second method we get for these 9 clusters

$$(1 + z_f) \approx 2.35(1 \pm 0.1) \approx 3.3(1 \pm 0.02)M_{13}^{-0.1}, \quad (38)$$

$$\langle B^{-1}(z_f) \rangle \approx 1.74(1 \pm 0.1).$$

To improve representativity of the subsample of 9 SPT clusters (37, 38) we can extend it up to 31 objects setting $\eta = 3.3$ for all objects with measured X-ray masses. This assumption agrees with inference (32) that for all clusters the pressure in central regions is almost the same and it weakly depends upon the virial masses and redshifts of formation of clusters. Thus for subsample of 31 clusters with $1 \leq M_{13} \leq 150$ we get

$$(1 + z_{obs}) = 1.66(1 \pm 0.15),$$

$$(1 + z_f) = \langle 3.3M_{13}^{-0.1} \rangle \approx 2.1(1 \pm 0.05), \quad (39)$$

$$\langle B^{-1}(z_f) \rangle = 1.66(1 \pm 0.1).$$

Similarity of these results and those obtained above for the subsample of 9 clusters (38) confirms validity of this approach.

4.3.3 Properties of REXCESS and Bolocam clusters

It is interesting to compare the pressure, density and redshift of formation, (37 & 38) with the same values obtained for 9 clusters of REXCESS survey (Arnaud et al. 2010; Pratt et al. 2010) with $10 \leq M_{13} \leq 75$

$$\langle P_c \rangle \approx 21.2(1 \pm 0.51)eV/cm^3, \quad (40)$$

$$\langle n_b \rangle \approx 0.33 \cdot 10^{-2}(1 \pm 0.54)cm^{-3}, \quad \langle \eta \rangle \approx 3.2(1 \pm 0.05),$$

$$(1 + z_f) \approx 2.3(1 \pm 0.1), \quad \langle B^{-1}(z_f) \rangle \approx 1.7(1 \pm 0.1). \quad (41)$$

Moderate differences of the pressure $\langle P_c \rangle$ observed in very different clusters (21, 32, 37, 40) demonstrate the high stability of these parameters. Unfortunately, for these clusters the central temperature was not measured so we have to use our estimates (26, 28) instead.

This comparison can be continued for the sample of 45 massive galaxy clusters imaged using the Bolocam for which pressure profiles were measured (Sayers et al. 2013). These clusters with masses $23 \leq M_{13} \leq 420$, temperature $4.4keV \leq \langle kT \rangle \leq 14keV$ and outer pressure $2.8eV/cm^3 \leq P_{500} \leq 14.9eV/cm^3$ are situated at redshifts $0.151 \leq z \leq 0.888$. For this sample the central pressure at $r \sim 0.07R_{500}$ is

$$\langle P_c \rangle \sim 50(1 \pm 0.2)eV/cm^3 M_{15}^{2/3} E^{4/3}(z), \quad (42)$$

with $E(z) = (1 + (1 + z)^3/3)$. For clusters with the mass $M_{15} \leq 1$ this result is also close to (32), (37), and (40). For these clusters the central temperature is also unknown and the central pressure is estimated with (26, 28).

4.4 Observed density profile of SPT clusters of galaxies

For all 83 objects of the SPT-catalogs the baryonic density slope α at a distance $r \simeq 0.04R_{500}$ is also measured and it is justly linked with the process of cooling of the compressed

gas. Here we confirm that this slope strongly correlates with the density of central regions of clusters,

$$\kappa(\alpha, n_b) \approx 0.76, \quad (43)$$

where the correlation coefficient κ is obtained according to (33). So strong correlation indicates that the steep profile is caused by the limited resolution of observations. Indeed the cold high density gaseous clouds naturally arise in the central regions of many clusters owing to significant density fluctuations that are enhanced by isobaric modes of the thermal instability. As was demonstrated in Doroshkevich, Zel'dovich (1981) peculiar motions of such clouds sometimes lead to their deformation and even complete disruption.

These results are fully consistent with conclusions of Arnaud et al. (2010) where similar entropy and density gradients were found for the set of REXCESS clusters. The close link between the power index and the baryonic density is indicated by their correlation coefficient.

5 OBSERVED PROPERTIES OF THE DM DOMINATED GALAXIES

Several DM dominated objects of galactic scale are known. These are the 41 dSph galaxies, 14 THING and 10 LSB galaxies. Analysis of these objects can be performed in the same manner as done above.

5.1 Observed properties of the dSph galaxies

During last years properties of dSph galaxies were discussed in detail in many papers. Thus, the main observed parameters of 28 dSph galaxies are listed and discussed in Walker et al. (2009, 2011), Penarrubia et al., (2010), and 13 And galaxies with similar properties are listed in Tollerud et al. (2012). These samples include objects in a wide range of masses, $0.1 \leq M_6 = M_{gal}/10^6 M_\odot \leq 100$, what allows us to reveal more reliably the mass dependence of their redshift of formation (Demiański & Doroshkevich 2014). In this case we have to deal with parameters of the central regions at the projected half-light radius but their reliability is limited and scatter is large. In spite of this it is interesting to compare characteristics of these galaxies with characteristics of clusters of galaxies presented in this Section and with theoretical expectations.

Thus for these galaxies we have for the central pressure, P_c , baryonic density, n_b , and entropy, S_b

$$\langle n_b \rangle \approx 28(1 \pm 0.78)M_6^{-0.5}cm^{-3}, \quad \langle \eta \rangle \approx 3.2(1 \pm 0.1),$$

$$\langle P_c \rangle \approx 28(1 \pm 0.9)eV/cm^3, \quad (44)$$

$$\langle S_b \rangle = 36(1 \pm 0.35)M_6^{0.87}eV \cdot cm^2.$$

It is important that in spite of large scatter of measured characteristics for these galaxies the pressure P_c (44) is quite similar to the pressure (21, 32, 37 & 40) found above for clusters of galaxies. As was discussed in Demiański & Doroshkevich (2014) these results agree well with expectations of simulations (Klypin et al., 2011) and reflect some important intrinsic properties of violent relaxation and formation of DM dominated virialized objects.

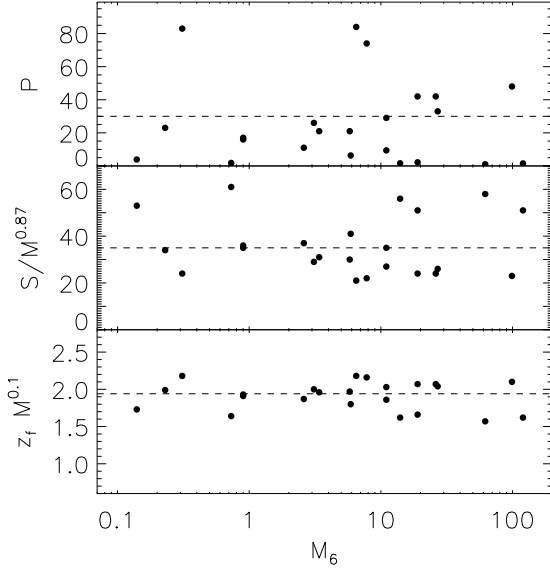


Figure 4. For 23 dSph galaxies functions P , $S/M_6^{0.87}$, and $\eta_6 = z_f M_6^{0.1}$ are plotted vs. the masses M_6 . Fits (44) & (45) are plotted by dashed lines

For the redshift of formation of the dSph galaxies we get (Demiański & Doroshkevich 2014)

$$\begin{aligned} \langle 1 + z_f \rangle &\approx 3.3(1 \pm 0.12) M_{13}^{-0.1}, \\ \langle B^{-1}(z_f) \rangle &\approx 2.4(1 \pm 0.12) M_{13}^{-0.1}. \end{aligned} \quad (45)$$

5.2 Direct estimates of mass of the DM particles

For clusters of galaxies the thermal velocities in central regions are $v_c \sim 100 - 1000 \text{ km/s}$ and they are clearly generated in the course of violent relaxation of the compressed matter. In contrast, the observed velocity dispersion of the dSph galaxies is not so large, $\sigma_{obs} \leq 10 \text{ km/s}$, what allows to obtain direct rough estimates of the velocity, free-streaming scale and mass of DM particles accumulated by these galaxies. One example of such estimates can be found in Boyarsky et al. (2009d) where for the mass of WDM particle four values were obtained in the range

$$m_{wdm} \geq 0.4 - 2.8 \text{ keV}. \quad (46)$$

Here we can get similar estimates using properties of low mass dSph galaxies with minimal velocity dispersions $\sigma_{obs} \sim 3 - 4 \text{ km/s}$.

Assuming that formation of these galaxies is accompanied by the adiabatic compression of weakly perturbed DM we can estimate the random velocities of the same population of DM particles before compression, σ_{homo} . For the four low mass dSph galaxies this velocity dispersion is

$$\sigma_{homo}(z=0) = \sigma_{obs} \left(\frac{\langle \rho_m(z=0) \rangle}{\rho_c} \right)^{1/3} \sim 0.01 \text{ km/s}, \quad (47)$$

and their comoving radius is

$$R_{homo} = (3M/4\pi\langle\rho_m(z=0)\rangle)^{1/3} \approx 11 \text{ kpc}. \quad (48)$$

The mass of these DM particles can be estimated from the temperature at the redshift when these particles become

non relativistic (Doroshkevich et al. 1980):

$$m_v c^2 \sim 3.5 k T_\gamma \frac{c}{\sigma_{homo}} \sim 22 \text{ keV}. \quad (49)$$

According to the estimates of Bardeen et al. (1986) for such particles the free-streaming scale is

$$R_f \sim (50 - 100) \text{ kpc} (1 \text{ keV}/m_v) \sim (2 - 5) \text{ kpc}, \quad (50)$$

what is even less than (48). The low precision of measurements of both σ_{obs} and ρ_c as well as a possible growth of σ_{obs} owing to the violent relaxation makes the estimates (47) and (49) very rough. Non the less, they demonstrate that probably among the population of cosmological DM particles there is a subpopulation with the mass (49) and the damping scale (50).

5.3 Observed properties of the THING and LSB galaxies

The number of observed DM dominated galaxies is very small and therefore we will use observations of all objects for which the influence of DM component is significant.

Here we consider 14 THING galaxies (de Blok et al. 2008) for which the contribution of DM component seems to be important. The virial mass of these galaxies can be roughly found from published rotation curves while estimates of their central density are given in de Blok et al. (2008). Similar estimates of mass and density of these galaxies are presented also in Chemin et al. (2011). However the central temperature of these galaxies is not known and further analysis is based on estimates (26, 28). Using relation (26) we can estimate the parameter η and redshift z_f for these 14 galaxies with the virial masses $5 \cdot 10^9 \leq M_{vir}/M_\odot \leq 7 \cdot 10^{11}$:

$$\langle \rho_c \rangle \approx 3.2 \cdot 10^{-2} (1 \pm 0.8) M_\odot / \text{pc}^3, \quad \langle \eta \rangle \approx 3.0(1 \pm 0.1),$$

$$\langle 1 + z_f \rangle \approx 5.0(1 \pm 0.2), \quad \langle B^{-1}(M_{vir}) \rangle \approx 3.7(1 \pm 0.2). \quad (51)$$

The central pressure and entropy for this sample can be found with (28) with large scatter

$$\langle P_c \rangle \approx 37(1 \pm 0.9) \text{ eV}/\text{cm}^3, \quad (52)$$

$$\langle S_c \rangle \approx 27 \text{ cm}^2 \text{ eV} (1 \pm 0.9),$$

which can be partly related to the stronger influence of the cooling process of baryonic component.

For the sample of LSB galaxies the masses and central densities are discussed in Kuzio de Naray et al. (2008). As before for these galaxies the central temperature was not measured and our analysis is based on estimates (26, 28). For 10 LSB galaxies with $10^9 \leq M_{vir}/M_\odot \leq 2 \cdot 10^{11}$ we get

$$\langle \rho_c \rangle \approx 2.7 \cdot 10^{-2} M_\odot / \text{pc}^3 (1 \pm 0.75), \quad \langle \eta \rangle \approx 3.1(1 \pm 0.1),$$

$$\langle 1 + z_f \rangle \approx 5.9(1 \pm 0.1), \quad \langle B^{-1}(M_{vir}) \rangle \approx 4.4(1 \pm 0.1). \quad (53)$$

Here the parameter η is determined by (25) and it coincides with the expected one. For this sample the central pressure and entropy can also be found with (28) with large scatter

$$\langle P_c \rangle \approx 14(1 \pm 0.8) \text{ eV}/\text{cm}^3, \quad (54)$$

$$\langle S_c \rangle \approx 19 \text{ cm}^2 \text{ eV} (1 \pm 0.7),$$

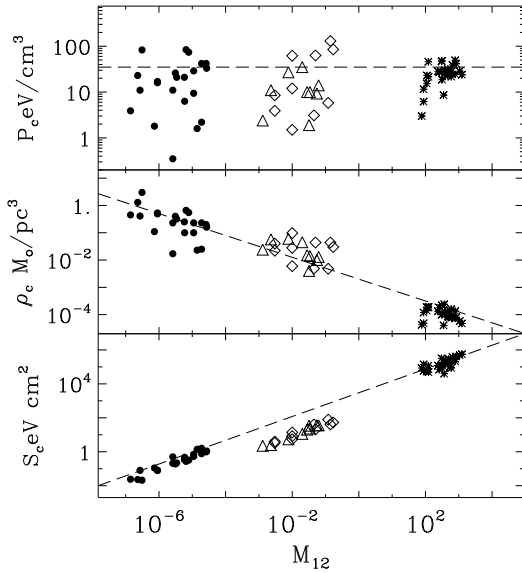


Figure 5. The central pressure, density and entropy of virialized DM dominated objects are plotted vs. mass for dSph (points), THING (triangle) and LSB (rhombus) galaxies and for 9 SPT and 18 nearby (21, 22) clusters of galaxies (stars) with x-ray masses and hot baryonic component. Fits (55) are plotted by dashed lines.

which also can be partly related to the stronger random influence of the cooling process of baryonic component.

It is necessary to bear in mind that for these objects the virial mass is underestimated while the central density and z_f are overestimated owing to the possible excess of baryons. Nonetheless the obtained value of $\langle \eta \rangle$ (51) and (53) shows that the final results are sufficiently reasonable.

These results for both THING and LSB galaxies are plotted in Fig. 5 & 6.

6 CENTRAL PRESSURE AND ENTROPY IN DM DOMINATED VIRIALIZED OBJECTS

Our analysis revealed some unexpected peculiarities in the internal structure of DM dominated virialized objects. First of them is a very weak dependence of the central pressure of such halos (21, 32, 37, 40, 42, 44, 52, & 54) on the virial mass, redshift of formation and other characteristics of these objects. In contrast, the central entropy of clusters of galaxies (22, 34, 35) significantly exceeds the entropy of DM dominated objects of galactic scale (44, 52, 54). For the dSph, THING and LSB galaxies and for 9 SPT (37) and 18 nearby (21, 22) clusters of galaxies the central observed pressure, P_c , density, ρ_c , and entropy, S_c are plotted in Fig. 5 and fitted by (55) :

$$\begin{aligned} P_c &\approx 36 \text{ eV/cm}^3, \quad \rho_c \approx 2 \cdot 10^{-3} M_{12}^{-0.4} M_\odot/\text{pc}^3, \\ S_c &\approx 3 M_{12}^{0.7} \text{ keV cm}^2, \quad M_{12} = M_{\text{vir}}/10^{12} M_\odot. \end{aligned} \quad (55)$$

The strong correlation of n_c & T_c together with weak correlation of P_c & S_c discussed in Sec. 4.3.2 confirm the objective character of these inferences

Of course these effects have only statistical significance what implies natural scatter of measured central pressures

and entropy and the parameter η (25). However both the limited precision of observations and the impact of cooling process of baryonic component significantly increase the random scatter of real measurements.

In order to explain so different behavior of central pressure and entropy it is necessary to remind that if the central pressure is determined mainly by the dynamical equilibrium of compressed DM dominated component then the central entropy includes two components, namely, the initial entropy of compressed matter and entropy generated in the course of compression and relaxation. The relative contribution of these components depends upon the halo mass and redshift of formation and our results indicate that the contribution of the first component progressively increases together with the virial mass of formed halos. This inference agrees with the well known regular growth of entropy with radius within virialized objects, $S \propto M_{\text{vir}} r$, what indicates the progressive generation of entropy in the course of matter relaxation. It is quite interesting to trace this behavior in more details in both observed and simulated clusters.

Thus first galaxies such as dSph ones are formed from cold DM particles and baryonic component with very low entropy (see, e.g. Demiański & Doroshkevich 2014). This implies that for these objects the central entropy of both DM and baryonic components (44) is mainly generated in the course of objects formation. In contrast, for later formed massive clusters of galaxies the contribution of initial entropy progressively increases and becomes more and more essential.

The initial entropy of baryonic component can be partly related to the progressive heating of intergalactic gas by ionizing UV background. For redshifts $z \leq 3$ when strong photoionization of HeI and HeII is caused by the hard UV radiation of quasars the entropy for slightly perturbed baryons and 3D Hubble expansion can be estimated as

$$T_b \sim 0.7 \text{ eV} (1+z)^{6/7}, \quad S_b \sim 18 (1+z)^{-8/7} \text{ cm}^2 \text{ keV}.$$

This entropy strongly exceeds the entropy of the THING and LSB galaxies and is more similar to the observed entropy of low mass clusters of galaxies. The Jeans mass of such baryonic component increases up to

$$M_J \approx 10^6 M_\odot \left(\frac{T}{10^4 \text{ K}} \right)^{3/2} \left(\frac{1 \text{ cm}^{-3}}{\langle n_{\text{bar}} \rangle} \right)^{1/2} \sim 10^{10} M_\odot (1+z)^{0.2},$$

and the formation of less massive objects is sharply decelerated.

At redshifts $z_f \geq 3$ the quasars contribution to ionizing UV radiation is small and the generated entropy of baryons depends upon the shape of more soft spectrum of the UV background. Thus the observed entropy of THING (52) and LSB (54) galaxies is similar to the entropy of dSph galaxies (44) what shows that for them the contribution of initial entropy is small. This means that probably at redshifts $z_f \geq 3$ the ionization of intergalactic gas is not accompanied by its essential heating.

On the other hand extraordinary efforts are required in order to increase the much more conservative entropy of DM component. As was noted above, perhaps, the progressive growth of small scale perturbations and their following randomization is the most promising way to increase the large scale entropy of both DM and baryonic components and to

explain the observed high entropy of clusters of galaxies. The problem requires further analysis in simulations.

The high stability of the central pressure for DM dominated objects was already noted in our previous paper (Demiański & Doroshkevich 2014) and here it is confirmed with wider observational base. It can be related to the combined influence of the violent relaxation and of the regular shape of the initial power spectrum of density perturbations and so, also velocity perturbations.

It is important that for the CDM model simulations show similarity of the dimensionless characteristics of DM halos such as the density and pressure profiles. In particular the density profiles are found to be close to NFW or Burkert (1995) ones with moderate variations of concentration $C \sim 3 - 5$. On the other hand the regular character of the CDM (Bardeen et al. 1986) and WDM (5) initial power spectra links together the virial mass of DM objects with their redshifts of formation and mean densities as this is demonstrated by Eqs. (25, 26, 28) and is discussed in the next Section. So the impact of the growth with time of the virial mass of formed objects is compensated approximately by corresponding drop of their mean density (see, e.g., (18, 26)).

7 MDM COSMOLOGICAL MODELS

Simulations show that characteristics of the virialized DM halos are much more stable than the characteristics of baryonic component and after formation at $z = z_f$ of virialized DM halos with $\langle \rho_{vir} \rangle \approx 18\pi^2 \langle \rho(z_f) \rangle$ slow matter accretion only moderately changes their characteristics (see, e.g., Diemer et al. 2013). Because of this, we can observe earlier formed high density galaxies with moderate masses even within later formed more massive but less dense clusters of galaxies, filaments and other elements of the Large Scale Structure. This means that using the model presented in Sec. 3 for description of the observed dSph, THING and LSB galaxies and clusters of galaxies dominated by DM component we can find one-to-one correspondence between their observed parameters and the so called redshift of object formation, z_f . Of course according to the Press – Schechter approach (Press, Schechter, 1974; Peebles 1974; Bond et al. 1991) these redshifts characterize the power spectrum of the density perturbation rather than the real period of the object formation.

Following the Press – Schechter ideas (7) we compare the function $\sigma_m(M)$ for various DM models with the observed function $B^{-1}(M_{vir})$ obtained in the previous Sections in a wide range of masses and redshifts. Such comparison allows us to quantify the influence of the DM particles on the rate of DM halos formation. Thus in Fig. 6 the function $B^{-1}(M_{vir})$ is plotted for the dSph, THING and LSB galaxies and for the sample of 31 clusters of galaxies (39) together with the function $\sigma_m(M_{vir})$ calculated for the standard CDM power spectrum, and for the MDM power spectrum (56) with σ_m obtained according to (13) for low massive WDM particles

$$p(k) = 0.27p_{cdm} + 0.73p_{wdm}(m_w), \quad m_w \approx 30\text{eV}, \quad (56)$$

and corresponding damping scale $M_{dmp} \sim 10^{14} M_\odot$. The

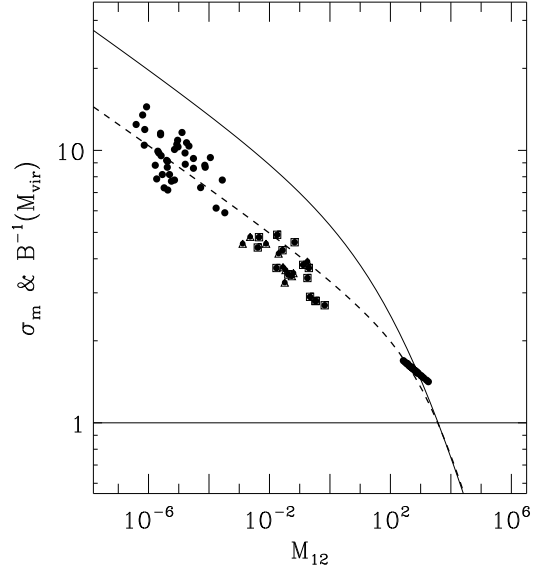


Figure 6. Correlation function of the matter density σ_m for the CDM power spectrum (11) and the combined spectrum (56) are plotted by solid and dashed lines. Function $B^{-1}(M_{vir})$ is plotted for the 41 dSph galaxies (left group of points) and for 31 clusters of galaxies from the SPT observed sample (right group of points). For 14 THINGS galaxies function $B^{-1}(M_{vir})$ is plotted by squares and for 10 LSB galaxies - by triangles.

functions $\sigma_m(M_{vir})$ are normalized using the cluster points (39).

Of course the observational base used in this discussion is very limited and it should be extended by adding observations of new objects with masses $M \simeq 10^{10} - 10^{12} M_\odot$, what may be crucial for determination of the real composition of dark matter. Unfortunately more or less appropriate estimates of the redshift z_f can be obtained mainly for DM dominated objects or for objects with clearly discriminated impact of DM and baryonic components. Here we use results obtained for 14 THINGS galaxies (de Blok et al. 2008) and 10 LSB galaxies (Kuzio de Naray et al. 2008). We hope that the list of possible appropriate candidates can be extended.

Next important problem is the reliability of the approach used in our analysis and obtained results. It depends upon the representativity of the observational data and is low because of the very limited available data and their significant scatter. Progress achieved during last years allows to begin discussion of MDM models but the low reliability of available observations is causing only qualitative character of our discussion. Indeed, the problem of estimates of the mass, density and other parameters of the observed objects is quite complex, methods used for such estimates are very rough and model dependent while their reliability is limited. Moreover the influence of baryonic component increases scatter of the measured parameters and makes it difficult to estimate the real precision of our results. Let us hope that because of the importance of this problem such observations will be extended and their precision improved.

On the other hand the simulated data are focused on clusters of galaxies, what is caused by the finite resolution of simulations. This limitation also does not increase reliability of our inferences. Non the less let us note that the analysis discussed in Sec. 4 is based on results of very large and high

quality simulations of the standard Λ CDM model (Klypin et al. 2011) which embraces relatively large accessible range of object masses and redshifts of formation.

As is seen from Figure 6 the standard CDM model cannot describe the system of observed points and, so, should be rejected. Quality of the WDM model with $m_w \approx 3\text{keV}$ is also limited and simulations (Shultz et al. 2014) show that in this model the objects formation at high redshifts is over-suppressed. Better description of observations is presented in Fig. 6 by the two component DM model with parameters (56).

The important result of our analysis is the demonstration of limited applicability of cosmological models with only one component power spectrum and great promises of models with more complex structure of the power spectrum. It is also important that the basic element of such complex power spectrum is the large contribution ($\sim 70\%$) of the low mass WDM spectrum with $m_w \sim 30\text{eV}$. It is noteworthy that after 30 years of absolute domination of the CDM model we return to more complex versions of the HDM models.

In turn such models imply existence of at least two damping scales one of which corresponds to the mass of clusters of galaxies, $M_{dmp} \sim 10^{13}M_\odot$. However such partial damping of the power spectrum leads only to a decrease of the rate of formation of less massive objects relatively to the standard CDM-like power spectrum.

Of course all these inferences are very preliminary. Thus, here we use the WDM power spectra with the transfer function (5) (Viel et al. 2005; Polisensky & Ricotti 2011; Marcovič & Viel 2013). More refined description of the MDM power spectrum and specially further progress in observations of DM dominated objects will change the best model parameters and estimates of masses and composition of the MDM model. Non the less even today replacement of some fraction of CDM particles by heavy WDM particles with $m_w \sim 10\text{keV}$ can be considered. Spectrum of such particles identified now (according to majority preference) as the sterile neutrinos can be included in (56) as a third component without noticeable changes of Fig. 6. Indeed, the available sample of observed DM dominated objects does not yet allow us to make any far-reaching conclusions about the actual properties of massive DM particles. However, the noticeable contribution of low mass WDM spectrum in (56) is crucial for the considered models

At the same time it is very important that the observed characteristics of objects are determined mainly by the linear combination of power spectra and so by the damping scales which in turn depend both upon particle masses and velocities. This means that the construction of the adequate complex cosmological model should include discussion of full DM evolution beginning from the period of inflation with estimates of the actual damping scales and transfer functions for all components allowing also for linear evolution of perturbations at $z \leq z_{eq}$. Simple example of such evolution is discussed by Boyarsky et al. (2009b) and in Sec. 2.3.

Thus, allowing for the decay of the separate components of power spectra according to (12) we can estimate the matter fractions of CDM and WDM components, f_{cdm} & f_{wdm} , for the model (56) with $g_{cdm} = 0.27$

$$f_{cdm} \approx 0.82, \quad f_{wdm} \approx 0.18. \quad (57)$$

Unexpectedly in spite of the relatively small value of g_{cdm}

the fraction of the CDM particles, f_{cdm} , remains significant as well as their influence upon the evolution of small scale objects. However the widely discussed controversial characteristics of DM objects such as the core-cusp problem, or number of low mass satellites depend upon the dissipative scale and the power spectrum rather than directly upon the mass or fraction of the CDM component. This supports the hope that these simpler problems also will be successfully resolved in the framework of the discussed MDM cosmological models.

These discussed complex intercorrelations produce additional problems for numerical simulations which now practically cannot simultaneously provide suitable size of computational box and required high mass resolution. This means that direct simulations with realistic complex power spectrum encounter many problems and require to use model simulations with subsequent rescaling procedures what makes difficult further comparison with observations. As usual the additional problem is the accurate description of possible impact of baryonic component.

So, more accurate simulations with various compositions of dark matter are required before we will have reliable inferences about properties of the DM component. These doubts are supported by moderate results of the first published simulations of the WDM cosmological models (Maccio 2012, 2013; Angulo, Hahn, Abel, 2013; Schneider, Smith & Reed, 2013; Wang et al. 2013; Libeskind et al. 2013; Marcovič & Viel 2013; Schultz et al. 2014; Schneider et al. 2014; Dutton et al. 2014).

8 CONCLUSIONS

In this paper we discuss two important problems of modern cosmology:

- (i) the composition of the dark matter,
- (ii) the internal structure of virialized DM dominated objects – the high stability of their central pressure and dependence of the central entropy upon mass and period of halos formation.

Summing up it is necessary to note that the proposed approach allows us to consider and to compare properties of DM dominated objects in an unprecedentedly wide range of masses $10^5 \leq M_{vir}/M_\odot \leq 10^{15}$. This comparison unexpectedly favors MDM models for which the domination of massive DM component is accompanied by a significant contribution of low mass DM particles. In turn in these models the power spectra of density perturbations at galactic scale significantly differ from the standard CDM-like ones.

Here we consider as a quite promising the MDM model for which the power spectrum is composed of fraction $g_{cdm} \sim 0.3$ of the CDM spectrum and fraction $g_{wdm} \sim 0.7$ of the WDM spectrum with low mass thermalized WDM particles and transfer function (5). The rough estimates of the mass fraction of these components are given by (57). Further progress can be achieved with more complex models with more realistic transfer functions instead of (5,13) and/or with replacement of some fraction of CDM particles by heavy WDM particles with mass $m_w \geq 3\text{keV}$ (such as the sterile neutrino).

We want to emphasize that unexpectedly in the spectrum (56) of this more promising MDM model the spectrum of low mass WDM particles with relatively large damping scale dominates. This can be considered as reincarnation in a new version of the earlier rejected HDM model. It is important that in the MDM model the impact of such low mass WDM particles decelerates the growth of perturbations and the rate of the objects formation for all objects with masses less than the low mass clusters of galaxies or massive galaxies, $M_{vir} \leq 10^{12} M_{\odot}$. However the contribution of CDM-like spectrum provides successful formation of low mass halos and other structure elements.

Further development of this approach could result in further complication of power spectra and in particular in introduction of an excess of power localized at small scale. Such modifications allow to essentially extend possibilities of the MDM models and even can allow to link the possible unexpected observed properties of some set of objects of galactic scales with peculiarities of the power spectrum. In some respect such an excess of power reminds the isocurvature models (see, e.g. Savelainen et al. 2013) with similar predictions and problems. However all such problematic multi parametric proposals should be considered in the context of general cosmological and inflationary models.

During the last decade the most reliable and interesting information about the power spectrum comes from observations of the perturbations at the period of recombination which are seen as the CMB fluctuations. Such observations are performed both with satellites (Komatsu et al. 2011; Larson et al. 2011; Ade et al. 2013) and the SPT and other ground telescopes (see, e.g., Saro et al. 2013). But they relate to large scales $L \geq 10 Mpc$ only. Limited information about the power spectrum at smaller scales can be obtained from observations of absorption spectra of distant quasars. But properties of such absorbers are very sensitive to spatial variations of poorly known ionizing UV background, what makes difficult interpretation of these observations and strongly limits their reliability.

The approach used in this paper for discussion of composition and properties of the DM particles is very indirect. We consider effects of strongly nonlinear multistep evolution of perturbations resulting in observed properties of the relaxed objects. The nonlinear evolution already leads to a strong loss of information about the primeval perturbations and composition of the DM component. These losses are further enhanced by the masking effects of dissipative evolution of the baryonic matter. To seek out the missing impact of the DM composition and primeval perturbations we have to compare observational data with numerical simulations majority of which are now focused on studying evolution of the standard Λ CDM models.

We used the general theory of gravitational instability for the DM objects to justify the expression (7) and Figure 6 and to quantify correlations between the virial mass of objects, M_{vir} , their redshift of formation, z_f , and the shape of the primordial power spectrum of perturbations (13) in a wide range of masses. In this respect our approach seems to be more helpful and informative than the earlier mentioned contradictions between the observed and simulated characteristics of the DM halos. Non the less it provides us with only preliminary qualitative inferences about the nature of DM particles and cosmological models.

It can be expected that another manifestation of the same interactions is the well known similarity of the internal structure of DM dominated virialized objects and, in particular, the high stability of the central pressure of these objects discussed in Secs. 4 & 6.

As is seen from Figs. 1 and 6 deviations between the CDM and MDM power spectra appear at scales $M_{vir}/M_{\odot} \sim 10^{12} - 10^{13}$. This means that properties of massive galaxies and clusters of galaxies such as their central pressure, entropy and specially the rate of formation are more sensitive to the composition of the dark matter and for impact of low mass particles. These possibilities were discussed in Sec. 6. Unfortunately published – and discussed in Secs. 4 and 5 – observations of such objects are limited and their interpretation is unreliable what do not allow us to reveal the expected effects. Additional problem is the impact of cooling of the baryonic component which masks the possible impact of the power spectrum and DM composition.

We believe that more detailed conclusions will be made on the basis of special simulations and after accumulation of more representative observational sample of high precision measurements of properties of DM dominated objects.

8.1 Acknowledgments

This paper was supported in part by the grant of president RF for support of scientific schools NS4235.2014.2. We thank S.Pilipenko, B.Komberg, A.Saburova and R.Rufini for useful comments. We wish to thank the anonymous referee for many valuable comments and suggestions.

REFERENCES

- Ade, P., et al. 2013, arXiv:1303.5076
- Agnese, R., et al. 2013, arXiv:1305.2405
- Anderhalden, D., Diemand, J., Bertone, G., Maccio, A., Shneider A., 2012, JCAP, 10, 047
- Angloher, G., et al., 2013, Eur.Phys.J., C72, 1971
- Arnaud, M., Pointecouteau, E., Pratt, G., 2005, A&A, 441, 893
- Arnaud, M., Pratt, G., Piffaretti, R., Böhringer, H., Croston, J., Pointecouteau, E., 2010, A&A, 517, 92; arXiv:0910.1234
- Angulo, R., Springel, V., White, S.D.M., Jenkins, A., Baugh, C., Frenk, C., 2012, MNRAS, 426, 2046
- Angulo, R., Hahn, O., Abel, T., 2013, arXiv:1304.2406
- Bardeen J.M., Bond J.R., Kaiser N., & Szalay A., 1986, ApJ, 304, 15
- Bennet C., et al., 2003, ApJS,, 148, 1
- Bernabei, R., et al., 2008, Eur.Phys.J., C56, 333
- Bernabei, R., et al., 2010, Eur.Phys.J., C67, 39
- Blumenthal, G., Faber, S., Primack, J., Rees, M., 1984, Nature, 311, 517.
- Bhattacharya, S., Habib, S., Heitmann, K., Vikhlinin, A., 2013, ApJ, 766, 32
- Bisnovaty-Kogan, G., & Novikov, I., 1980, Astr.Zh., 57, 899
- Bode, P., Ostriker, J., Turok, N., 2001, ApJ, 556, 93
- Bond, R., Efstathiou, G., Silk, J., 1980, Phys.Rev.Lett., 45, 1980
- Bond, R., Szalay, A., 1983, ApJ, 274, 443
- Bond R. & Szalay A., 1984, ApJ, 274, 443;
- Bond, R., Cole, S., Efstathiou, G., Kaiser, N., 1991, ApJ, 379, 440
- Borde, A., Palanque-Delabrouille, N., Rossi, G., Viel, M., Bolton, J., Yèche, C., Le Goff, J.-M., Rich, J., 2014, arXiv:1401.6472
- Bovill, M, Ricotti, M., 2009, ApJ, 693, 1859

- Boyarsky, A., Lesgourgues, J., Ruchayskiy, O., Viel, M., 2009a, JCAP, 05, 012
- Boyarsky, A., Lesgourgues, J., Ruchayskiy, O., Viel, M., 2009b, PhRvL, 102t1304
- Boyarsky, A., Ruchayskiy, O., Shaposhnikov, M., 2009c, ARNPS, 59, 191
- Boyarsky, A., Ruchayskiy, O., Iakubovskiy D., 2009d, JCAP, 0903, 005
- Boyarsky, A., Iakubovskiy D., Ruchayskiy, O., 2013, arXiv:1306.4954
- Boyarsky, A., Ruchayskiy, O., Iakubovskiy D., Franse, J., 2014, arXiv:1402.4119
- Boylan-Kolchin, M., Bullock, J., Kaplinghat, M., 2012, MNRAS, 422, 1203
- Branchesi, M., Gioia, I., Fanti, C., Fanti, R., 2007, A&A, 472, 739
- Bryan, G., Norman, M., 1998, ApJ, 495, 80
- Bulbul, E., Markevitch, M., Foster, A., Smith, R., Loewenstein, M., Randall, S., 2014, arXiv:1402.2301
- Bullock, J., Kolatt, T., Sigad, Y., Somerville, R., Kravtsov, A., Klypin, A., Primack, J., Dekel, A., 2001, MNRAS, 321, 559
- Burenin, R., Vikhlinin, A., 2012, Astronomy Lett., 38, 1
- Burkert A., 1995, ApJ, 447, L25
- Carr, B., 2014, arXiv:1402.1437
- Chemin, L., de Blok, W., Mamon, G., 2011, AJ, 142, 109
- Choi, K.-Y., Kim, J., Roszkowski, L., 2013, 1307.3330
- Collins, M., et al., 2014, ApJ, 783, 7
- Costanzi, M., Villaescusa-Navarro, F., Viel, M., Xia, J.-Q., Borgani, S., Castorina, E., Sefusatti, E., 2013, JCAP, 12, 012
- Croston, J., et al., 2008, A&A, 487, 431
- Cyr-Racine, F.-Y., Sigurdson, K., 2013, Phys.Rev.D, 87, 103515
- Dayland, T., Finkbeiner, P., Hooper, D., Linden, T., Portillo, S., Rodd, N., Slatyer, T., 2014, arXiv:1402.6703
- de Blok, W., Walter, F., Brinks, E., Trachternach, C., Oh, S.-H., Kennikutt, R., 2008, AJ, 136, 2648
- Demiański, M., Doroshkevich, A., 1999, ApJ, 512, 527
- Demiański, M., Doroshkevich, A., 2004, A&A, 422, 423
- Demiański, M., Doroshkevich A., & Turchaninov, V., 2006, MNRAS, 372, 915
- Demiański, M., Doroshkevich, A., Pilipenko, S., Gottlöber, S., 2011, MNRAS, 414, 1813.
- Demiański, M., Doroshkevich A., 2014, MNRAS, 439, 179.
- Diemand, J., Kuhlen, M., Madau, P., 2007, ApJ, 667, 859
- Diemer, B., More, S., Kravtsov, A., 2013, ApJ, 766, 25
- Dipak, M., Cole, P., Viel, M., 2012, MNRAS, 427, 2359
- Doroshkevich, A., Khlopov, M., Sunyaev, R., Zel'dovich, Ya., 1980, SvAL, 6, 252
- Doroshkevich, A., Khlopov, M., Sunyaev, R., Szalay, A., Zel'dovich, Ya., 1980, Proc. 10th Texas Symposium on Relativistic Astrophysics, Ann.New York Acad. Sci., 375, 32.
- Doroshkevich A., Zel'dovich Ya., 1981, JETP, 80, 801
- Doroshkevich, A., Khlopov, M., 1984, MNRAS, 211, 277.
- Doroshkevich, A., Khlopov, M., Kotok, E., 1986, SvA., 30, 251
- Doroshkevich, A., Klypin, A., Khlopov, M., 1988, SvA., 32, 127
- Doroshkevich A., Naselsky, I., Naselsky, P., Novikov, I., 2003, ApJ., 596, 709
- Doroshkevich A., Lukash, V., Mikheeva, E., 2012, PhyU., 55, 3
- Dreves, M., 2013, J.Mod.Phys. E, 22, 1330019
- Dutton, A., Maccio, A., 2014, arXiv:1402.7073
- Eisenstein, D., Hu, W., 1998, ApJ., 496, 605
- Feng, J., 2010, ARA&A, 48, 495
- Ferrer, F., Hunter, D., 2013, JCAP, 09, 005
- Fillmore J.A., & Goldreich P., 1984, ApJ, 281, 1
- Foëx et al., 2013, A&A, in press, arXiv:1208.4026
- Gaibelli, R., 2014, ARNPS, 54, 315
- Grishchuk, L., Zeldovich, Ya., 1981, SvA., 25, 267
- Governato, F. et al., 2012, MNRAS, 422, 1231
- Gurevich, A., Zybin, K., 1995, Phys.Usp., 38, 687
- Hinshaw G., et al., 2013, ApJS, 208, 19
- Horiuchi, S., Humphrey P., Onorbe, J., Abazajian, K., Kaplinghat, M., Garrison-Kimmel, S., 2013, arXiv:1311.0282
- Khedekar, S., Churazov, E., Kravtsov, A., Zhuravleva, E., Lau, E., Nagai, D., Sunyaev, R., 2013, MNRAS, 431, 954
- Klypin, A., Trujillo-Gomez, S., Primack, J., 2011, ApJ, 740, 102; arXiv:1002.3660
- Kollmeier, J., et al., 2014, arXiv:1404.2933
- Komatsu, E., et al. 2011, ApJS, 192, 18
- Koposov, S., Yoo, J., Rix, H.W., Weinberg, D., Maccio, A., Escude, J., 2009, ApJ, 696, 2179
- Kravtsov, A., Borgani, S., 2012, ARA&A, 50, 353
- Kusenko, A., Phys.Rep., 2009, 481, 1
- Kusenko, A., Rosenberg, L., 2013, 1310.8642
- Kuzio de Naray, R., Mcgaugh, S., de Blok, W., 2008, ApJ, 676, 920
- Laporte, C., Walker, M., Penarrubia, J., 2013, MNRAS, 433, 54L
- Larson, D., et al. 2011, ApJS, 192, 16
- Libeskind, N., Di Cintio, A., Knebe, A., Yepes, G., Gottlöber, S., Steinmetz, M., Hoffman, Y., Martinez-Vaquero, L., 2013, arXiv:1305.5557
- Lithwick Y., Dalal N., 2011, ApJ, 734, 100L, arXiv:1010.3723;
- Lloyd-Davies, E., 2011, MNRAS, 418, 14
- Loeb, A., Barkana, R., 2001, ARA&A, 39, 19
- Ludlow, A. et al., 2013, MNRAS, 432, 1103L
- Maccio, A., Paduroiu, S., Anderhalden, D., Schneider, A., Moor, B., 2012, MNRAS, 424, 1105
- Maccio A., Ruchayskiy O., Boyarsky A., Munos-Cuartas J., 2013, MNRAS, 428, 882
- Mantz, A., Allen, S., Rapetti, D., Ebeling, H., 2010, MNRAS, 406, 1759
- Marcovič, K., Viel, M., 2013, arXiv:1311.5223
- McDonald, M., et al., 2013, ApJ, 774, 23
- Medvedev, M., 2014, Phys.Rev.Let., 113, 071303
- Meiksin, A., White, M., Peacock, J., 1999, MNRAS, 304, 851
- Mikheeva, E., Doroshkevich A., Lukash, V., 2007, NCimB, 122, 1393
- Modak, R., Majumdar, D., Rakashit, S., 2013, arXiv:1312.7488
- Moughan, B., Giles, P., Randall, S., Jones, C., Formen, W., 2011, arXiv:1108.1200
- Nagai, D., Kravtsov, A., Vikhlinin A., 2007, ApJ, 668, 1
- Navarro J.F., Frenk C.S., & White S.D.M., 1995, MNRAS, 275, 720
- Navarro J.F., Frenk C.S., & White S.D.M., 1996, ApJ, 462, 563
- Navarro J.F., Frenk C.S., & White S.D.M., 1997, ApJ, 490, 493
- Nulsen, P., Powell, S., Vikhlinin, A., 2010, ApJ, 722, 55
- Peacock, J., Heavens, A., 1990, MNRAS, 243, 133
- Peebles P.J.E., 1967, ApJ, 147, 859
- Peebles P.J.E., 1974, ApJ, 189, L51
- Peebles P.J.E., Seager, S., Hu, W., 2000, ApJ, 539, L1
- Penarrubia, J., Navarro, J., McConnachie, A., 2008, ApJ, 673, 226
- Penarrubia, J., Pontzen, A., Walker, M., Koposov, S., 2012, ApJ, 759L, 42
- Penarrubia, J., Benson, A., Walker, M., Gilmore, G., McConnachie, A., Mayer, L., 2010, MNRAS, 406, 1290
- Pilipenko, S., Doroshkevich, A., Lukash, V., Mikheeva, E., 2012, MNRAS, 427L, 30
- Pointecouteau, E., Arnaud, M., Pratt, G., 2005, A&A, 435, 1
- Polisensky E. & Ricotti M., 2011, PhRvD, 83.043506
- Pontzen, A., & Governato, F., 2014, Nature, 506, 171,
- Prada, F., Klypin, A., Cuesta, A., Betancort-Rijo, J., Primack, J., 2012, MNRAS, 423, 3018
- Pratt, G., Arnaud, M., Pointecouteau, E., 2006, A&A, 446, 429
- Pratt, G., Croston, J., Arnaud, M., Böhringer, H., 2009, A&A, 498, 361
- Pratt, G., et al., 2010, A&A, 511, A85
- Press, W., Schechter, P., 1974, ApJ, 187, 425

- Primack, J., 1984, Enrico Fermi International Scoole of Physics, Varenna, Italy.
- Reinhardt, C., et al., 2013, *ApJ*, 763, 127
- Rubakov, V., 2011, *PhyU*, 54, 633
- Ruel J., et al., 2013, arXiv:1311.4953
- Ruffini R., Arguëlles, C., Rueda, J., 2014, in press.
- Saliwanchik, B., et al. arXiv:1312.3015
- Samushia, L., et al., 2014, *MNRAS*, 439, 3504
- Saro, A., et al., 2013, arXiv:1312.2462
- Savelainen, M., Valiviita, J., Walia, P., Rusak, S., Kurki-Suonio, H., 2013, *PhRvD*, 88, 063010.
- Sawala, T., Frenk, C., Crain, R., Jenkins, A., Schaye, J., Theuns, T., Zavala, J., 2013, *MNRAS*, 431, 1366
- Sayers, J., et al., 2013, *ApJ*, 768, 177
- Schneider, A., Smith, R., Reed, D., 2013, *MNRAS*, 433, 1573
- Schneider, A., Anderhalden, D., Maccio, A., Diemand, J., 2014, *MNRAS*, 441, L6
- Schultz, C., Onorbe, J., Abazajian, K., Bullock, J., 2014, arXiv:1401.3769
- Souza, R., Mesinger, A., Ferrara, A., Haiman, Z., Perna, R., Yoshida, N., 2013, arXiv:1303.5060 γ 2keV
- Suhada, R., et al., 2012, *A&A*, 537, 39, 1076, arXiv:1111.0141
- Tasitsiomi, A., Kravtsov, A., Gottlöber, S., Klypin, A., 2004, *ApJ*, 607, 125
- Teyssier, R., Pontzen, A., Dubois, Y., Read, J., 2013, *MNRAS*, 429, 3068
- Tollerud et al., 2012, *ApJ*, 752, 45
- Trimain, S., Gunn, J., 1979, *PRL*, 42, 407
- Turner, M., Steigmann, G., Krauss, L., 1984, *Phys.Rev.Let.*, 52, 2090.
- Umemura, M., Loeb, A., Turner, E., 1993, *ApJ*, 419, 459
- Verde, L., Feeney, S., Mortlock, D., Peiris, H., 2013, *JCAP*, 09, 13
- Viel, M., Lesgourgues, J., Haehnelt, M., Matarrese, S., Riotto, A., 2005, *PhRvD*, 71f3534
- Viel, M., Becker, G., Bolton, J., Haehnelt, M., 2013, *PhRvD*, 88d3502
- Vikhlinin, A., Kravtsov, A., Forman, W., Jones, C., Markevitch, M., Murrey, S., Van Speybroeck, L., 2006, *ApJ*, 640, 691
- Vikhlinin, A., et al., 2009, *ApJ*, 692, 1033
- Villaescusa-Navarro, F., Marulli, F., Viel, M., Branchini, E., Castorina, E., Sefusatti, E., Saito, S. 2013, arXiv:1311.0866
- Walker, M., et al. 2009, *ApJ*, 704, 1274
- Walker, M., Penarrubia, J., 2011, *ApJ*, 742, 20
- Walker, M. 2012, arXiv:1205.0311
- Wang, M.-Y., Croft, R., Peter, A., Zentner, A., Purcell, C., 2013, 1309.7354
- Wise, J., & Abel, T., 2008, *ApJ*, 685, 40
- Wyman, M., Rudd, D., Vanderveld, R., Hu, W., 2014, *PRL*, 112, 051302
- Zel'dovich Ya.B., 1970, *A&A*, 5, 84
- Zel'dovich Ya.B., Novikov I.D., 1983, *Structure and evolution of the Universe*, University of Chicago Press.
- Zhang, Y., Böringer, H., Finoguenov, A., Ikebe, Y., Matsushita, K., Schueker, P., Guzzo, L., Collins, C., 2006, *A&A*, 456, 55